

Prevailing Trends Modelled by a Small-World Network

Shin'ya Yamada and Syuji Miyazaki*

Graduate School of Informatics, Kyoto University, 606-8501, Japan

We extended a network model of scientific paradigm shifts proposed by S. Bornholdt et al. (2011) to one of prevailing trends, such as music CDs. A mean-field state-update rule was replaced by a local state-update rule that depends only on nearest neighbors of a small-world network. Then, we used the extended model to establish a connection between the model and theories in social sciences. In particular, we used the ideas of the diffusion of innovations and early adopters introduced by Everett M. Rogers, and a chasm pointed out by Geoffrey A. Moore. Finally, we used real commercial data of music CDs. We showed that sales of the music CDs of major and independent labels can be modeled using the original lattice model and our small-world network model, respectively.

1. Introduction

We report our results related to complex networks, which currently have attracted considerable attention in physics, mathematics, engineering, and social sciences.¹⁾ Researchers also discuss the interrelations between complex networks and nonlinear science. We have provided examples of associations among chaos, fractal, and small-world networks.^{2,3)} One of the authors also discussed random walks on the Watts–Strogatz small-world network⁴⁾ and large-deviation statistics on a social networking service.⁵⁾

In this study, we numerically examined prevailing sociopsychological trends using a small-world network model. We demonstrated sociological notions such as the diffusion of innovations and early adopters introduced by Rogers⁶⁾ and a chasm described by Moore.⁷⁾ The lattice model of scientific paradigm shifts reported by Bornholdt et al.⁸⁾ has the following characteristics: (1) a scholar interacts with the four nearest-neighbor scholars on a square lattice; (2) a scientific paradigm accepted by a scholar is accepted by a nearest-neighbor scholar with a probability proportional to the ratio of the number of scholars accepting that paradigm to the number of all scholars; (3) an existing paradigm is never reproduced. We describe this model in the first half of Sect. 2.

We extended the above-mentioned model as follows. (1) The terminology of cellular automata was used. The interaction range is given by the von Neumann neighborhood (square lattice with four neighbors). We replaced it with the Moore neighborhood (square lattice plus diagonals with eight neighbors). Then, we easily obtained the cluster coefficient of the Watts–Strogatz small-world network model by constructing a triangular lattice. (2) The Moore neighborhood (link) was rewired analogously to the Watts–Strogatz model. Some of the Moore neighborhood was replaced by the short-cut neighbors. (3) A scientific paradigm accepted by a scholar was accepted by the nearest-neighbor scholar with a probability proportional to a function of the ratio of the number of directly connected scholars accepting the same paradigm to the total number of directly connected scholars. A function in the form of a Fermi distribution function in the field of quantum statistical mechanics has two parameters: inverse temperature (the degree of synchronization) and chemical potential (threshold

above which a scholar easily accepts the paradigm accepted by the nearest-neighbor scholars), as shown later in Eq. (1). This modification enabled us to generalize a scholar accepting a specific scientific paradigm to an ordinary person who has a specific opinion, is infected by a specific contagion disease, and is purchasing a specific music CD, as described in the latter half of Sect. 2. The method of diffusion depends on the update rule.

Diffusion of innovations was first explained in the book written by Everett M. Rogers.⁶⁾ He stressed the importance of the early adopter. In addition, Moore introduced the notion of crossing a chasm.⁷⁾ In Sect. 3, we verify these diffusion of innovation, early adopter, and crossing the chasm concepts using the extended network model. In the *mean-field* update rule, the network structure does not affect the diffusion. The local update rule depends strongly on network structures. For example, major-label music CDs are sold with aggressive promotion and high advertising costs, while independent-label CDs might be recommended among enthusiastic admirers. The former and latter roughly correspond to the mean-field update rule and the local update rule, respectively.

In Sect. 4, we used the sales data of major- and independent-label music CDs on the commercial website Amazon Japan. We compared the original lattice model and the extended small-world model. Section 5 is devoted to the concluding remarks.

2. Update Rules on Small-world Networks

We extend the agent-based model on a square lattice by Bornholdt et al.⁸⁾ Their model is intended to describe scientific paradigm shifts. We first quote their model description: *The model is defined on a 2-d square lattice with $N = L^2$ agents. Each agent i is assigned a number r_i which can take any integer value. This number plays the role of a particular idea or concept. At any time step one random agent i is selected, and the following two actions are attempted: (i) One of the nearest neighbors j to the agent i is selected. Denoting by n_j the total number of agents with integer value equal to that of j , we with probability n_j/N let the agent i change its integer value to that of its neighbor j , provided that i never assumed that particular integer value before. In case it had, then no update is made. (ii) With probability α another random agent k is assigned a new random integer which does*

*miyazaki.syuji.8m@kyoto-u.ac.jp

not appear anywhere else in the system. Thus α represents the “innovation” rate.⁸⁾ According to their abstract, their model exhibited a fairly regular pattern of global paradigm shifts, where older paradigms are eroded and subsequently replaced by new ones.⁸⁾ The above-mentioned update rule (i) implies that the change takes place only on the nearest neighbor. We extend their model, introducing shortcuts and a small-world network. Scientific paradigms, new products, etc., diffuse not only locally but also globally and irregularly. In this model, we observe a variety of spatiotemporal evolution patterns, as shown later in Fig. 10. Later in this section, we incorporate psychological peer pressure. We also introduce a biased update rule with a nonlinear logistic function (Eq. (1)).

Bornholdt and his colleagues considered four static undirected links between the nearest neighbors on a square lattice under periodic boundary conditions. We added the four links between the second nearest neighbors in order to incorporate small-worldness. Therefore, we considered undirected links between eight Moore neighborhoods on a square lattice. Then, we rewired the links with a rewiring probability p , as in the Watts–Strogatz model. In Fig. 1, we plotted the clustering coefficient C and the mean path length L against the rewiring probability. The p dependences on C and L are similar to those in the original Watts–Strogatz model.⁹⁾ A small-world network is a type of mathematical graph. Most nodes are not neighbors. The neighbors of any given node are likely to be neighbors of each other. Most nodes can be reached from other nodes within a small number of hops. More specifically, the model satisfies $C(p)/C(0) \sim 1$ and $L(p)/L(0) \ll 1$. Many empirical graphs have a small-world nature, including social networks and gene networks.⁹⁾

We define a discrete dynamical variable $x(i)$ on node i . Bornholdt and his colleagues considered the variable as a scientific paradigm. We extend this idea and consider the variable to be hit songs, opinions, and commercial products. One can consider a variable $x(i)$ as a label of different scientific paradigms, songs, opinions, products, etc. The original mean-field update rule consists of two parts. For a fixed node i and a randomly chosen neighbor j , the value of $x(i)$ is replaced by $x(j)$ with a certain probability that is given by the ratio of the number of nodes having the same value as $x(j)$ in the entire system to the number of all nodes (mean-field update rule). The index i runs from 1 to the system size N . The propagation of opinions or products is modelled in this way. We modelled the creation of a new opinion or product in accordance with the original model. For a randomly chosen node i , the dynamical variable $x(i)$ takes a new value with probability α . The new value is never equal to any value appearing in the entire system thus far. One can consider this to indicate a newly released music CD. We introduce the following variables and parameters.

s : The cumulative number of a specific value of $x(i)$. The value is adopted by nodes ($i = 1, 2, \dots, N$) from its emergence to its extinguishment. s satisfies $1 \leq s \leq N$. The cumulative adoption rate is given by s/N .

$\sigma(i)$: The cumulative number of a specific value of $x(i)$ directly connected to node i at a certain time.

N_1 : The number of nodes that take the most adopted value of x at a certain time, which is time-dependent. N_1 satisfies $1 \leq N_1 \leq N$.

q : The number of alternations of the most adopted value of x during the entire observation time range.

S_{\max} : The maximum value of N_1 during a time range in which a single value of x is dominant.

$\langle S_{\max} \rangle$: The average of S_{\max} over q different values of dominant x values.

θ : The threshold beyond which we consider a value of x is diffused over the system ($0 < \theta \leq 1$).

l : The number of cases satisfying $N_1/N > \theta$ during the entire observation time range. We can consider l to be the number of hit products, hit songs, etc.

T : The time difference between the subsequent cases satisfying $N_1/N > \theta$. We can regard T to be the lifetime of a hit product, hit song, etc.

$\langle T \rangle$: The average of T over l different values.

Important parameters are the rewiring probability p as in the Watts–Strogatz model and the number of new dynamical variables per unit time.

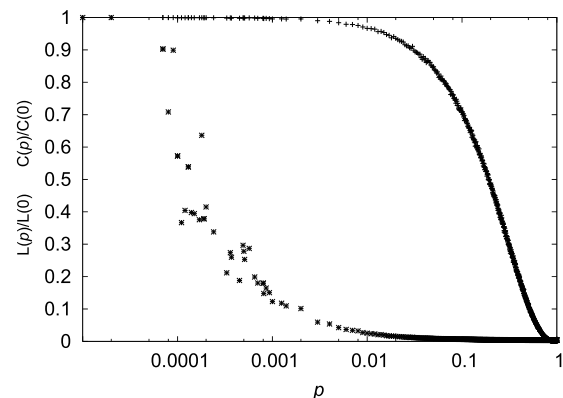


Fig. 1. Rewiring rate dependencies of the clustering coefficient (+) and mean path length (*).

We introduce another extension. This is not for network structures, but for a mean-field property. To reflect social networks, we extended the model to depend on network structures. We compared the results obtained using our extended model with the social-science theories about early adopters and a chasm, as described in the next section.

In Fig. 2 (upper), the value of $x(i)$ (\diamond) is replaced with another value (\heartsuit). The transition probability from $x(i)$, indicated by \diamond in the upper panel of Fig. 2, to $x(i)$ shown as \heartsuit is given by the function $f(r)$ of r , in which r is given by the number of the \heartsuit nodes $\sigma(j)$ directly connected to node j before the update divided by the total number of nodes directly connected to node j , or the degree of node j , $k(j)$. In this case, we have $\sigma(j) = 2$, $k(j) = 8$, and, $r = 2/8$. In other cases, $\sigma(j)$ is equal to four, one, and one for \bullet , \circ , and \circ nodes, respectively. The transition probability is proportional to $f(r)$ given by the nonlinear logistic function with two parameters H and μ :

$$f(r) = \frac{1}{1 + \exp[-H(r - \mu)]}, \quad r = \frac{\sigma(j)}{k(j)}. \quad (1)$$

Two parameters, H and μ , are respectively referred to as the synchronization intensity and synchronization threshold. The

H dependence of the logistic function is shown in Fig. 2 (middle, lower) for $H = 3$ and $H = 20$. For a small H , the logistic function is nearly linear with respect to the ratio r . For a large H and a larger ratio r than the threshold μ , the transition probability is nearly equal to unity, thus μ is termed the synchronization threshold.

Here, we stress the need for introducing the above-mentioned logistic function. Solomon Asch conducted a psychology experiment and reported the existence of a threshold above which the human population makes it easier for an individual to accept a majority opinion.^{10,11} It was also suggested that the threshold was determined not by the absolute number of the majority, but by its relative ratio. Prevailing trends are sociopsychologically positioned as social synchronization phenomena. First, a new product or opinion first is gradually adopted at an early stage. Then, explosive growth is observed in a specific group above the threshold. Finally, the new product jumps to other groups and spreads throughout the entire population. The parameter μ in the logistic function is our mathematical realization of the sociopsychological threshold.

We present trend curves for nine sets of parameters based on the modified model in Figs. 3–5, in which the total number of nodes with the most dominant dynamical variable s is plotted against the number of simulation time steps. Important parameters are the rewiring probability p defined in the Watts–Strogatz model and the number of new dynamical variables per unit time αN , which is given by the new product creation rate α multiplied by the system size N . Figures 3, 4, and 5 correspond to the number of new products $\alpha N = 0.1, 4,$ and 10 ($N = 3600$), respectively. The upper, middle, and bottom panels correspond to the rewiring probability $p = 0, 0.2,$ and 1 , namely, a regular lattice, small-world network, and random network, respectively. These trend curves depend both on αN and the rewiring probability p , in contrast to the original mean-field update rule.

The synchronization intensity (H) dependence of the average adoption rate $\langle S_{\max} \rangle$ as a function of αN is shown in Fig. 6 (upper, middle). The case of weak intensity ($H = 3$) is shown in the upper panel. The three symbols correspond to the three different network structures: regular lattice (+), small-world network (\times), and random network (*). In rewired networks, the size of the dominant variable is larger than that without rewiring ($p = 0$). The case of strong intensity ($H = 20$) is shown in the middle panel. The values of \times with $H = 20$ are larger than those of + and * for $\alpha N > 1$. This is not the case when $H = 3$.

The synchronization threshold (μ) dependence of the average adoption rate $\langle S_{\max} \rangle$ as a function of αN is shown in the lower panel of Fig. 6. The three symbols correspond to the three different values of the synchronization threshold, $\mu = 2/8$ (+), $3/8$ (\times), and $4/8$ (*). The optimal threshold μ is nearly equal to $3/8$ at which the dominant nodes easily cover the entire system. For too large or too small μ , the dominant nodes often fail to cover the entire system completely.

For an optimal threshold μ and a strong intensity H , whose concrete values are given as $\mu = 3/8$ and $H = 20$, we first consider the size distribution of all clusters at a specific value of $\alpha N = 0.363$. As shown in the upper panel of Fig. 7, the three different bars correspond to the three different network structures: no rewiring ($p = 0$, vertical rectangles), small-world

($p = 0.2$, light gray bars), and full rewiring ($p = 1$, dark gray bars). For a regular lattice without rewiring, the cluster size is concentrated at smaller values. In the case of a small-world network, the cluster size distributes most widely from a small value to a large value.

The number of new products whose adoption rate exceeds 4% of the system size during the entire simulation, l , was plotted against αN [Fig. 7 (middle)]. Note that the threshold θ in the middle panel of Fig. 7 is equal to 4%. It has a single maximum. Symbols +, \times , and * correspond to a regular lattice, small-world network, and random network, respectively. As shown in the lower panel of Fig. 7, the average duration of the top product $\langle T \rangle$ plotted against αN has a single minimum. The maximum and minimum values depend on the rewiring probability p . Among the different network structures, the largest maximum of the top product and the smallest average duration of the top product are obtained in the case of a small-world range of p . The extrema are located in the range of αN between 0.1 and 1.

The small-world network with a large H yields a larger $\langle S_{\max} \rangle$, larger l , and shorter $\langle T \rangle$ than those of other networks, which can be regarded to indicate increased circulation of hit products, as suggested in Figs. 6 (upper, middle) and 7 (middle, lower).

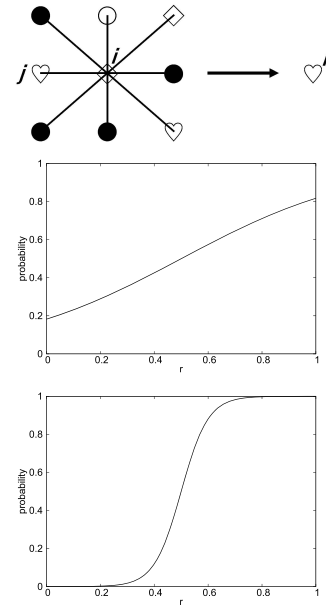


Fig. 2. (Upper) Illustration of our modified update rule. The middle node (\diamond) has eight neighbors and two nodes (\heartsuit) are connected. The transition probability from \diamond to \heartsuit is given by Eq. (1), the function of $r = \sigma(j)/k(j)$, $f(r)$. Different symbols correspond to different values of $\sigma(j)$. In this case of the transition from \diamond to \heartsuit , $\sigma(j) = 2$, the degree of node j , $k(j)$, is 8, and $r = 2/8$. (Middle and lower) Transition probability plotted against the ratio r for $\mu = 0.5$ and $H = 3$ (middle) and for $\mu = 0.5$ and $H = 20$ (lower).

3. Comparison with Diffusion of Innovations Theory

First, we will briefly review some social science notions. Diffusion of innovations is a theory that seeks to explain how, why, and at what rate new ideas and technology spread through cultures, as proposed by Everett M. Rogers.⁶ In the

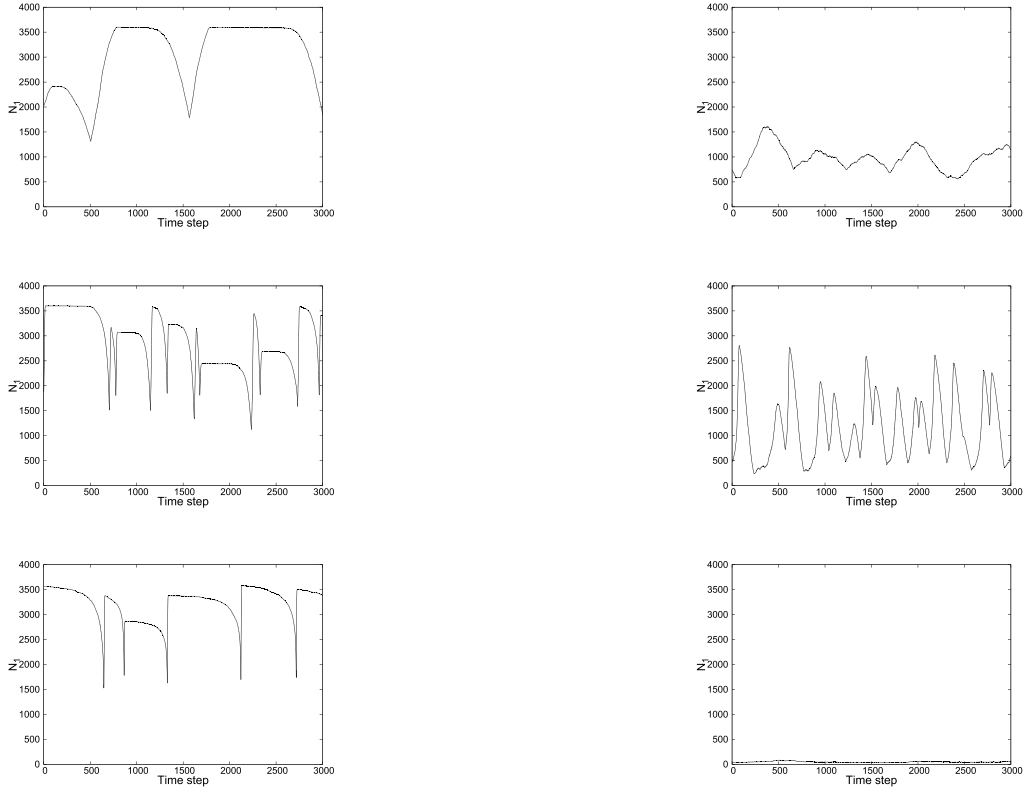


Fig. 3. Total number of nodes with the most dominant dynamical variable s is plotted against the number of simulation time steps. We set the number of new products per unit time $\alpha N = 0.1$, $N = 3600$, $H = 20$, and $\mu = 3/8$ in our modified update rule. The rewiring rate is fixed as $p = 0$ (top), 0.2 (middle), and 1 (bottom). The instantaneous top product is switched at a local minimum (cusp), for example, the 500th time step for $p = 0$ (top panel).

Fig. 5. The same as Fig. 3 except $\alpha N = 10$.

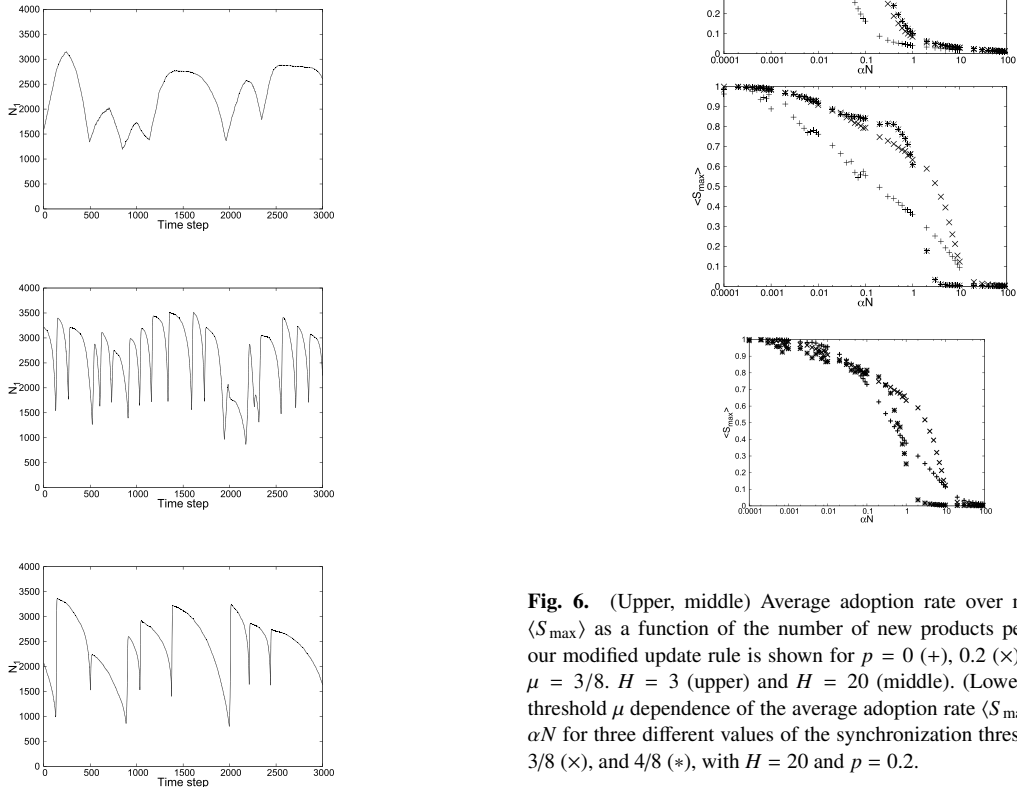


Fig. 4. The same as Fig. 3 except $\alpha N = 4$.

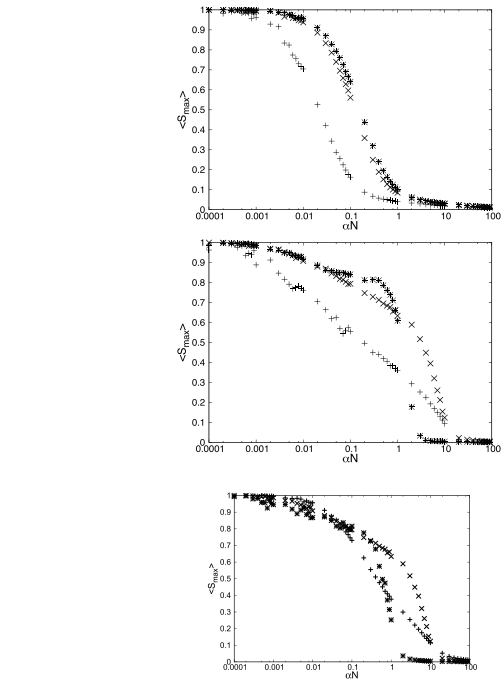


Fig. 6. (Upper, middle) Average adoption rate over many top products $\langle S_{\max} \rangle$ as a function of the number of new products per unit time αN in our modified update rule is shown for $p = 0$ (+), 0.2 (x), and 1 (*) and for $\mu = 3/8$. $H = 3$ (upper) and $H = 20$ (middle). (Lower) Synchronization threshold μ dependence of the average adoption rate $\langle S_{\max} \rangle$ as a function of αN for three different values of the synchronization threshold, $\mu = 2/8$ (+), $3/8$ (x), and $4/8$ (*), with $H = 20$ and $p = 0.2$.

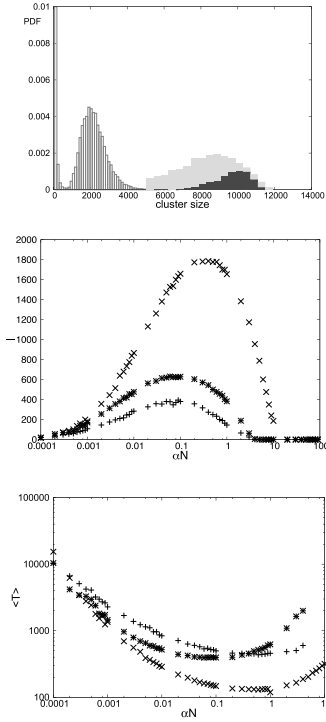


Fig. 7. (Upper) Size distribution of all clusters at a specific value of $\alpha N = 0.363$ ($N = 12100$) for three different network structures: no rewiring ($p = 0$, vertical rectangles), small-world ($p = 0.2$, light gray bars), and full rewiring ($p = 1$, dark gray bars). The gray bars are shown only for the cluster size larger than 5000 ($p = 0.2$ and 1). (Middle) Number of clusters larger than 4% of the system size as a function of αN for no rewiring ($p = 0$, +), small-world ($p = 0.2$, \times), and full rewiring ($p = 1$, *) over 250000 time steps. (Lower) Average duration of the top product (T) plotted against αN for no rewiring ($p = 0$, +), small-world ($p = 0.2$, \times), and full rewiring ($p = 1$, *) for $N = 3600$. We set $H = 20$ and $\mu = 3/8$.

theory, five successive groups of consumers adopt a new technology. We confine ourselves to a hit product. The number of consumers as a function of time of purchase since the launch of the product follows the bell curve. People are divided into five categories. The first 2.5% of consumers, for example, consumers who buy the new model of a smartphone on the launch date, are called innovators. The next 13.5% of consumers are called early adopters. These two categories of consumers amount to 16%. Around 16% of all consumers present a barrier to occupying the whole market. Geoffrey A. Moore termed this barrier the chasm. The following 34%, 34%, and 16% are respectively referred to as the early majority, late majority, and laggards, respectively. The cumulative number of purchasers implies the market share. Its temporal dependence follows an S-shaped curve, as shown in the upper panel of Fig. 8.

For Fig. 8 (lower), we selected the first two top products from among all products using our extended model with $H = 20$, $\mu = 3/8$, $N = 3600$, and $\alpha N = 0.01$ in the case of the small-world network ($p = 0.2$). The number of instantaneous adopters of the top product as a function of time has a single maximum. The first top product emerges approximately at the 300th time step and ends approximately at the 1500th time step. At this time step, the next top product emerges.

In Fig. 9 (upper), the instantaneous adoption rate $\Delta s/S_{\max}$

of the top product as a function of time from time step 550 to 680 is magnified. The five categories, from innovators to laggards, are separated by vertical lines in the case of the small-world network ($p = 0.2$) (bars) for the first top product in Fig. 8 (lower). The S-shaped cumulative adoption rate or market share, s/S_{\max} , as a function of time is also shown (crosses). Note that s is the number of nodes of the top product and $\Delta s/S_{\max}$ is the difference of s in the unit of time steps.

The cases of no rewiring ($p = 0$) and full rewiring ($p = 1$) are shown in the middle and lower panels of Fig. 9, respectively. In the case of a regular network without rewiring, the adoption rate curve is highly symmetric. In contrast, the adoption rate as a function time in two rewired cases ($p = 0.2$ and $p = 1$) grows slowly at the innovator and early adopter steps. After the chasm, which may be termed the 16% barrier, it grows markedly from the early majority to the laggard steps.

For a specific top product that covers the entire network, diffusion of the product is illustrated by using snapshots for the three different network structures, no rewiring ($p = 0$), small-world ($p = 0.2$), and full rewiring ($p = 1$), in Fig. 10. The five colors correspond to the five categories from innovators to laggards, as shown in Fig. 9.

In the case of a regular network without rewiring, the product diffuses in the form of wave propagation, as shown in the upper panel of Fig. 10, in which a snapshot is shown at the time step corresponding to the late majority category. The empty area is filled with other products at this time step. Thereafter, the green (x -shaped) late majority area grows and the laggard part falls into the empty area such that the area is filled with the five colors (grayscale intensities). In the case of a small-world network, islands of many sizes correspond to the five categories distributed over the entire system, as shown in the middle panel of Fig. 10, which shows a snapshot at the time step corresponding to the eventual laggard category. The top product covers the entire network at this time step. In the full rewired random network, the color (grayscale intensity) of the node is independently changing and no finite-size island of a specific color (grayscale intensity) can be found, as shown in the lower panel of Fig. 10, which shows a snapshot at the time step corresponding to the eventual laggard category. The top product covers the entire network at this time step.

In the discussions thus far, one of the top products was described. However, most new products vanish before attaining a large adoption rate. Probability densities are plotted as a function of the largest adoption rate of each product using our modified model with $H = 20$, $\mu = 3/8$, $\alpha N = 0.08$, $N = 12100$, $\alpha = 6.6 \times 10^{-6}$ [$p = 0$ (+), 0.2 (\times)], and $\alpha N = 1.0$, $\alpha = 8.3 \times 10^{-5}$ [$p = 1$ (*)], as shown in Fig. 11. All probability density functions have a minimum adoption rate between 20% and 80%. For a value smaller than the minimum value of s/N , the PDF monotonically and algebraically decreases. The power exponent is nearly equal to -1.4 . For a larger value of s/N , a larger realization probability is noted. Thus, the value of minimum s/N , which is not exactly equal to 16%, is a kind of barrier against realization across the entire system. This is the chasm in our modified model.

4. Real Data

In this section, we compared real data with the results of our extended model. We acquired data from the top 100 rank-

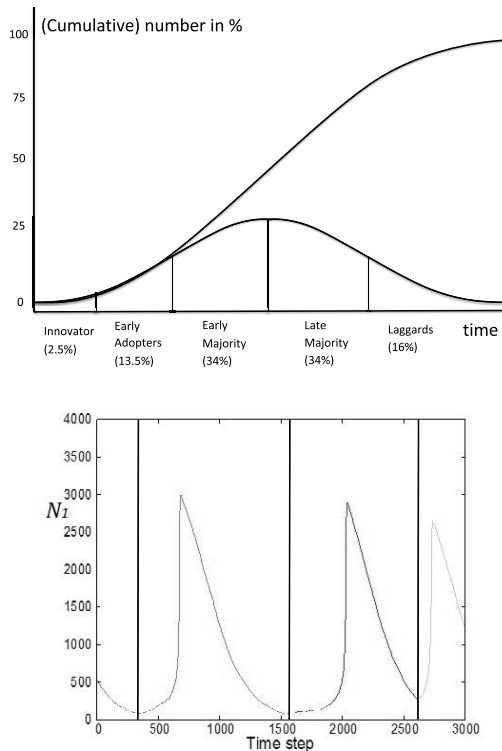


Fig. 8. (Upper) Number of customers as a function of time of purchase from a product’s launch (bell curve). The curve has a single maximum. Cumulative number of customers as a function of time (S-shaped curve). (Lower) Instantaneous adoption number of the top product as an asymmetric function of time for our modified network model in the case of a small-world network ($p = 0.2$). Switches of top products are indicated by vertical lines.

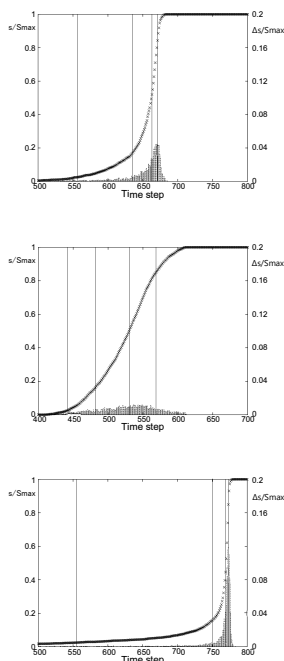


Fig. 9. (Upper) Instantaneous adoption rate $\Delta s/S_{\max}$ (right axis) of the top product as a function of time from time steps 550 to 680 is magnified. Five categories from innovators to laggards are separated by vertical lines in the case of a small-world network ($p = 0.2$). The S-shaped cumulative adoption rate or market share, s/S_{\max} (left axis), as a function of time is also shown. (Middle) $p = 0$. (Lower) $p = 1$.

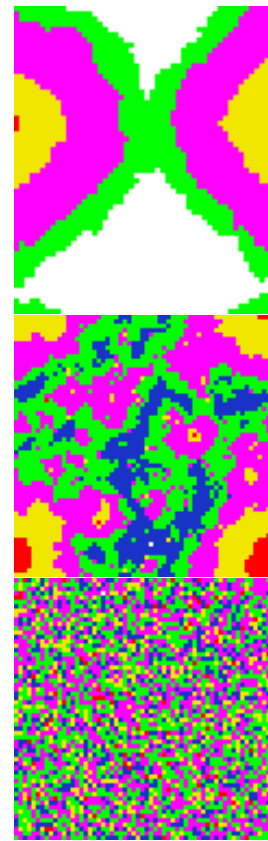


Fig. 10. (Color online) (Upper) Visualization of the square lattice. For the case of a regular lattice without rewiring ($p = 0$), a snapshot in the late majority period is shown. The colored (gray) region is filled with a top product. Colors (grayscale intensities) correspond to the five categories from innovators to laggards. The blank area is filled with other products. (Middle) Small-world network ($p = 0.2$). (Lower) Random network ($p = 1$).

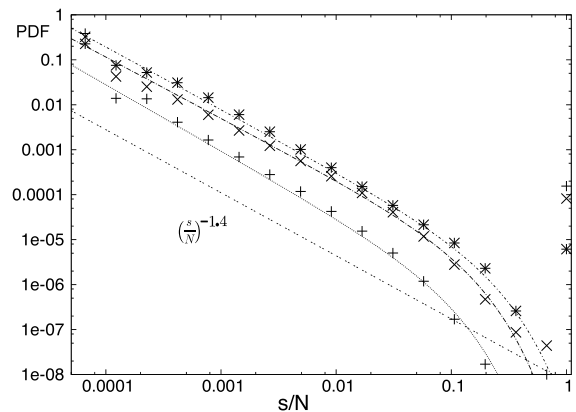


Fig. 11. Probability density functions are plotted as double logarithmic plots against the largest adoption rate of each product for $H = 20$, $\mu = 3/8$, and $\alpha N = 0.08$ [$p = 0$ (+), 0.2 (×)] and $\alpha N = 1.0$ [$p = 1$ (*)]. The power law with the exponent -1.4 is shown (dashed straight line).

ing of the music CD branch of the Amazon Japan website (<http://www.amazon.co.jp>) in November 2013. We compared major-label and independent-label pop music CDs. In Fig. 12 (upper), we plot cumulative distributions against duration in the top 100 ranking. We normalize the duration by the average duration. Major-label CDs climb up earlier

than independent-label CDs but are subsequently overtaken by independent-label CDs.

Major-label CDs have a larger market. They have high advertising costs invested in mass media. We can describe this situation by simulation using the mean-field Bornholdt–Jensen–Sneppen model. We set $N = 10000$ and $\alpha = 2 \times 10^{-7}$ ($\alpha N = 0.002$). The model resembles the real data. Independent-label CDs have a smaller market. Lower advertising costs are invested. Social networks of enthusiastic fans are important for independent-label CDs. We can describe this situation by simulation using our model. We set $\alpha N = 0.09$ ($N = 3600$ and $\alpha = 2.5 \times 10^{-5}$), $H = 20$, $\mu = 3/8$, and $p = 0.2$. Our model resembles the real data. We found a set of parameters that resemble the real data for the two situations shown in the middle panel of Fig. 12. We found these settings by happenstance. In Fig. 12 (lower), we show a double logarithmic plot of the upper panel of Fig. 12. Note that the exponents of the power laws are different in the growing time range. We assume that the exponent depends on the network structure. On a regular lattice, we consider the bulk of a hit product composed of n nodes. The size of the perimeter is proportional to \sqrt{n} . We have $\frac{dn}{dt} \propto \sqrt{n}$, i.e., algebraic growth. In the case of a hit product on a complicated network, the growth rate $\frac{dn}{dt}$ might be proportional to n , i.e., exponential growth. Fractal growth with a different power exponent might be possible.

5. Concluding Remarks

In Sect. 2, we extended the mean-field Bornholdt–Jensen–Sneppen model to sensitively reflect the network structure. We also incorporated the psychological peer pressure into our model with a simple expression.

In Sect. 3, we compared theories in social sciences and our simulation model. We used the diffusion of innovation theory and the chasm theory. We can regard the chasm as the minimum points in Fig. 11 around $0.1 < s/N < 1$. The power law distributions for smaller s/N values correspond to numerous minor products. The rightmost points in Fig. 11 correspond to hit products. Note that Bornholdt et al.⁸⁾ first reported that the distribution consists of a power-law distribution and a rightmost point. Roger’s adoption curve appears as the part of the waveform of the single top product from its emergence as the top product to the subsequent emergence of the next top product, as shown in Figs. 3–5. In the previous study, using their update rule,⁸⁾ the adoption curve showed an abrupt increase. Using our update rule, we obtained different forms of the adoption curve. The forms reflect the numerous network structures (shown in Figs. 3–5).

In Sect. 4, we found that our results resembled real data of the Japanese major and independent music market. The data could be simulated using the Bornholdt–Jensen–Sneppen model and our model. The important point is that the growth of the cumulative distribution of the duration in top 100 ranking follows power laws with different exponents, which are assumed to reflect the different network structures.

- 1) A. Barrat, M. Barthlemy, and A. Vespignani, *Dynamical Processes on Complex Networks* (Cambridge University Press, Cambridge, U.K., 2012).

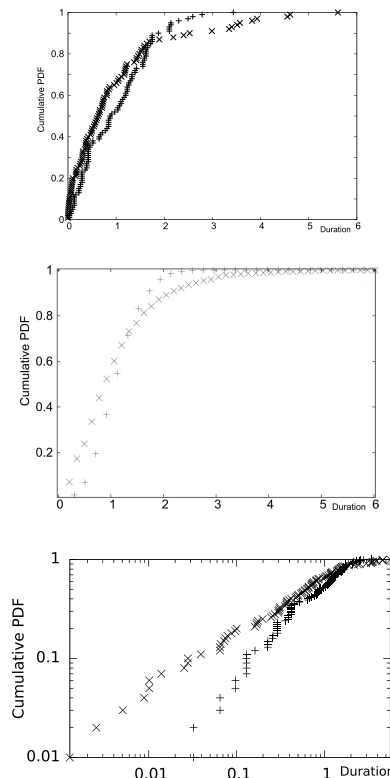


Fig. 12. (Upper) Durations of major-label (\times) and independent-label ($+$) CDs in top 100 ranking. Cumulative distributions are plotted against the duration normalized by the average duration. (Middle) Data of major-label and independent-label CDs can be approximated by the mean-field Bornholdt–Jensen–Sneppen model (\times) and our model ($+$) with a suitable set of parameters. Cumulative distributions are plotted against the duration normalized by the average duration. (Lower) Double logarithmic plot of the upper panel. Major-label (\times) and independent-label ($+$) CDs.

- 2) X. S. Yang, Phys. Rev. E **63**, 046206 (2001).
 3) X. S. Yang, Solitons and Fractals **13**, 215 (2002).
 4) T. Takaguchi and S. Miyazaki, Forma **24**, 37 (2009).
 5) T. Takaguchi, K. Ejima, and S. Miyazaki, Prog. Theor. Phys. **124**, 27 (2010).
 6) E. M. Rogers, *Diffusion of Innovations* (Free Press, New York, 2003) 5th ed.
 7) G. A. Moore, *Crossing the Chasm: Marketing and Selling High-Tech Products to Mainstream Customers* (Harper Business Essentials, New York, 1991).
 8) S. Bornholdt, M. H. Jensen, and K. Sneppen, Phys. Rev. Lett. **106**, 058701 (2011).
 9) D. J. Watts and S. H. Strogatz, Nature **393**, 440 (1998).
 10) S. E. Asch, Sci. Am. **193**, 31(1955).
 11) D. J. Watts, *Six Degrees: The Science of a Connected Age* (W. W. Norton, New York, 2004).